RESEARCH ARTICLE

Synchronization of a Seven-Term Chaotic 4D System Using a Simplified Fixed-Time Adaptive Integral Nonsingular Terminal Sliding Mode Control and Its Circuit Realization

NAPASOOL WONGVANICH[ID], (Member, IEEE), PITCHAYANIN MOONMUANG, NATCHANAI ROONGMUANPHA[ID], AND WORAPONG TANGSRIRAT[ID]

School of Engineering, King Mongkut's Institute of Technology Ladkrabang (KMITL), Bangkok 10520, Thailand

Corresponding author: Worapong Tangsrirat (worapong.ta@kmitl.ac.th)

ABSTRACT This work presents an adaptive gain fixed-time synchronization of a seven-term hyperchaotic 4D system, along with its analog circuitry realizations. To facilitate a simplistic circuit realization of the closed loop system, the control design process initiates with the design of a novel, simplified fixed-time stability lemma that gives a lower convergence time, while being easier to compute. A nonlinear, fixed-time adaptive-gain nonsingular terminal sliding mode controller was then designed to synchronize the hyperchaotic 4D system. Theoretical analyses successfully achieved fixed-time synchronization, and computer simulations verified the achievement of zero-error convergence across all states within 1 second, irrespective of the initial conditions and even in the presence of significant parameter and disturbance changes. Analog circuitry implementations of the adaptive gain fixed-time chaotic synchronization configuration were realized using commercially available components, for instance, LF357 and AD633. The circuit equations were devised to replicate those used in the controller, with the goal of facilitating troubleshooting by ensuring simplicity. Electronics workability was tested using PSPICE simulation program. The results demonstrated that active synchronization was achieved in fixed time with less than 1% error across the states in the presence of disturbances. Finally, the developed fixed-time chaotic synchronization was applied to a secure communication system. The results indicate that the original and recovered messages exhibit a high degree of similarity to each other after a fixed duration of 1 second.

INDEX TERMS Chaotic synchronization, adaptive gain fixed-time control, terminal sliding mode control, closed-loop circuit implementation.

I. INTRODUCTION

Since the seminal discovery of the Lorenz system [1], chaos theory has experienced continuous growth over the past three decades. Chaotic systems have many characteristics of interest, from their well-known pronounced sensitivity to initial conditions, randomness, and non-periodicity [2], and to their relevance in many natural phenomena, from

The associate editor coordinating the review of this manuscript and approving it for publication was Ludovico Minati[ID].

atmospheric convection, which was the discovery of the Lorenz system [1], to electronic circuits [3]. Since the days of the classical Lorenz and Sprott systems, researchers have also discovered continuous streams of chaotic systems. Some of the examples include [4], [5], [6], [7], [8].

Chaos synchronization has been in the limelight of recent chaotic research, requiring the use of various control algorithms, ranging from traditional linear feedback control [9], [10], and adaptive and optimal controls [11], [12], [13], [14]. Nonlinear and backstepping control methods

have also been designed, for example [15], [16], [17], [18]. Another advanced technique, such as adaptive sliding mode control, was designed in [19]. The conventional integral sliding mode controller adds the integral action to the system state variables. This gets rid of steady-state errors and makes the system more robust overall [20]. In [21], the construction of a cubic sliding mode controller was reported to synchronize the chaos.

The earlier asymptotic stability designs in the literature are somewhat limited. That is, even though stability is guaranteed, the convergence time is not bounded and cannot be determined by the control engineers. The concept of finite-time stability was then proposed in [22]. In [23], the researchers developed an adaptive controller with the aim of suppressing chaotic vibrations in gyroscopes within a specified time. A finite-time synchronization of a chaotic system was designed via the sliding mode control framework in [24], [25], and [26].

Nevertheless, the settling time of a finite-time control is intricately linked to the initial states. This implies that, if the initial conditions happen to be large enough, the settling time would also be large, since the convergence rates would ultimately be reduced. Hence, it is not possible to achieve a unified and specified convergence time by utilizing the finite-time control strategy. For this very reason, the concept of a fixed-time control scheme was proposed [27]. The fixed-time stability retains the features of the finite-time stability, with the exception that the time itself can be expressed by selecting only the appropriate control parameters. This new control strategy has recently gained traction with recent works developing on the work of Polyakov [28], [29]. Fixed-time output feedback control for a double integrator system was designed in [30]. The work conducted by [31] further explored the concept of fixed-time output control for higher-order integrator systems. Other applications of the fixed-time control are seen in [32], [33], and [34].

The work of Polyakov in [27] introduced the fixed-time stability condition $\dot{V} \leq -a_1 V^{\alpha} - a_2 V^{\beta}$. Since then, other fixed-time stability notions have also been proposed. The work of Chen [35] designed the fixed-time stability condition $\dot{V} \leq -a_1(t) V^{\alpha} - a_2 V^{\beta} - c$. Chen then modified the previous condition to read $\dot{V} \leq a_1 V^{\alpha} - a_2 V^{\beta} - a_3 V$ [28]. An alternative fixed-time stability notion includes $\dot{V} = \frac{p}{qT} \frac{V^{1-\frac{q}{p}}}{1-\tanh^2(\frac{q}{p})}$ [36]. It is evident that the complexity of fixed-time stability conditions has significantly escalated over time. Consequently, a controller developed based on these complicated stability conditions is inevitably intricate, posing challenges, particularly with regards to electronic circuit implementations.

The heart of chaotic secure communication lies in the ability of a chaotic system to generate unpredictability that makes it challenging to reproduce and predict. Chaotic secure communication methods generally involve chaotic masking, chaotic modulation, and chaotic shift keying [37].

Although chaotic modulation does give a more secure performance, it also requires a significantly higher channel signal-to-noise ratio (SNR) [38]. Chaotic masking involves adding a chaotic signal generated by the chaotic system to the information signal at the transmitter end, while later subtracting the synchronized chaotic signal from the received signal at the receiver end. This process thus focuses on the active synchronization of chaos. In this respect, many approaches have existed; some examples include adaptive control methods [39], impulsive control [40], backstepping and sliding mode control methods [21], [41], [42]. Finite-time chaotic synchronization was previously designed in [26]. Designing an adaptive fixed-time controller for a disturbed chaotic system remains an interesting research topic, where the overarching objective of this design is to incorporate a practical circuit implementation, a facet that has not been addressed in existing literature. Note also that the design of [26] was too complicated and could not cope with disturbances. The aim of this work is to attain a less intricate electronic realization of active chaotic synchronization for a disturbed 4D chaotic system through the design of a simpler adaptive fixed-time controller that also uses a newer, simplified fixed-time stability lemma. The fixed-time synchronization is further illustrated by a chaotic masking secure communication application.

The main contributions and features of this work are as follows:

1) The design of a newer fixed-time stability lemma that is more precise and simpler than the previous popular fixed-time stability lemmas. Moreover, the convergence time estimation is simpler to compute than the ones used in popular fixed-time stability lemmas.

2) The design of a nonlinear, fixed-time adaptive gain nonsingular terminal sliding mode synchronization of the seven-term disturbed hyperchaotic 4D system that is simpler to implement. A theoretical proof is given, demonstrating a faster reaching time (T_{reach}) than the earlier works of [43] and [44].

3) The realization of the closed-loop response under the effect of disturbances through analog circuitry is easier to implement than the ones designed in [26], along with its application in secure communications applications.

The paper is now organized as follows: Section II offers the preliminaries and gives the new simplified fixed-time stability lemma. In Section III, the adaptive fixed-time integral terminal sliding mode control for the synchronization of the seven-term chaotic system is designed. The implementation of the circuit is described in Section IV. The conclusion of this work is drawn in Section VI.

II. PRELIMINARIES AND THE SIMPLIFIED FIXED TIME STABILITY LEMMA

This section thus outlines the general control problem formulation with some lemmas and theorems relating to the presented control design strategy.

Definition 1 (Fixed-Time Stability) [45]: A nonlinear dynamical system given by:

$$\dot{x} = f(x), \quad x(0) = x_0, \quad (1)$$

is termed fixed-time stable if there exists a settling time T_s, for any arbitrary initial condition, satisfying:

$$\lim_{t \to T_s} ||x(t)|| = 0, \text{ and } ||x(t)|| = 0, \quad \text{for all } t \ge T_s \quad (2)$$

where T_s is a settling time and $|| \cdot ||$ denotes the Euclidean norm.

Lemma 1 [46]: The following inequality holds for some k, l > 0 and a, b > 1 such that $\frac{1}{a} + \frac{1}{b} = 1$:

$$kl \le \frac{k^a}{a} + \frac{l^b}{b}. \quad (3)$$

Lemma 2 [29]: For a continuous differentiable positive definite radially unbounded $V(x)$ such that:

$$\dot{V}(x) \le -aV^{\rho_1} - bV^{\rho_2}, \quad (4)$$

for some a, b > 0, $0 < \rho_1 < 1$ and $\rho_2 > 1$. System (1) is global fixed-time stable with the settling time given by:

$$T_s \le \frac{1}{a}\left(\frac{a}{b}\right)^{\frac{1-\rho_1}{\rho_2-\rho_1}}\left(\frac{1}{1-\rho_1} + \frac{1}{\rho_2-1}\right). \quad$$

Proof: The proof of this lemma is given in [29]. □

Lemma 3 [28]: If there exists a continuous differentiable positive definite radially unbounded V such that:

$$\dot{V} \le -aV^{\rho_1} - bV^{\rho_2} - cV, \quad (5)$$

for some a, b, c > 0, $0 < \rho_1 < 1$ and $\rho_2 > 1$. The dynamics of (1) achieve fixed-time stability with the settling time given by:

$$T_s \le \frac{1}{c(1-\rho_1)}\ln\left(1 + \frac{c}{a}\right) + \frac{1}{c(\rho_2-1)}\ln\left(1 + \frac{c}{b}\right). \quad (6)$$

Proof: The proof of this lemma is given in [28]. □

Lemma 4: Suppose there exists a radially unbounded, continuous positive definite V satisfying:

$$\dot{V} \le -a_1(a_2V + a_3V^\beta)^2 V^{-\beta}. \quad (7)$$

for some $a_1, a_2, a_3 > 0$, $1 < \beta < 2$ and $V = 0 \implies x = 0$, then system (1) achieves fixed-time stability with the settling time given by:

$$T_s \le \frac{1}{a_1a_2a_3(\beta-1)}. \quad (8)$$

Proof: Note that the expression given in (7) can easily be rearranged to:

$$\frac{1}{(a_2V + a_3V^\beta)^2} V^\beta \, dV = -a_1 \, dt. \quad (9)$$

Now, let $u = a_2V$ and $v = (a_2V + a_3V^\beta)$, then $du = a_2 \, dV$ and $dv = (a_2 + a_3\beta V^{\beta-1}) \, dV$. Let us now attempt to evaluate the following quantity:

$$\frac{u \, dv - v \, du}{v^2} = \frac{a_2V(a_2 + a_3\beta V^{\beta-1})dV - a_2(a_2V + a_3V^\beta)dV}{(a_2V + a_3V^\beta)^2}$$
$$= \frac{a_2a_3(\beta-1)V^\beta \, dV}{(a_2V + a_3V^\beta)^2}. \quad (10)$$

It then follows that:

$$\frac{V^\beta}{(a_2V + a_3V^\beta)^2} \, dV = \frac{1}{a_2a_3(\beta-1)}\left[\frac{u \, dv - v \, du}{v^2}\right],$$
$$= \frac{1}{a_2a_3(\beta-1)} \, d\left(\frac{u}{v}\right). \quad (11)$$

As a result of (11), we get

$$d\left(\frac{u}{v}\right) = -a_1a_2a_3(\beta-1) \, dt. \quad (12)$$

Integrating both sides of (12) yields:

$$\frac{u}{v} = \frac{u_0}{v_0} - a_1a_2a_3(\beta-1)t$$
$$= \frac{a_2V(0)}{a_2V(0) + a_3V(0)^\beta} - a_1a_2a_3(\beta-1)t. \quad (13)$$

If the time t is chosen such that:

$$t = \frac{1}{a_1a_2a_3(\beta-1)} \frac{a_1V(0)}{a_2V(0) + a_3V(0)^\beta}. \quad (14)$$

Then it can be deduced that:

$$\frac{a_1V(0)}{a_2V(0) + a_3V(0)^\beta} = 0, \Leftrightarrow V = 0 \text{ if } x = 0, \quad (15)$$

thereby implying that V is indeed monotonically decreasing in $t \in (0, \infty)$. Thus, there must exist a settling time T_s such that $V = 0$. We can estimate such time by:

$$T_s < \frac{1}{a_1a_2a_3(\beta-1)} \frac{a_2V(0)}{a_2V(0) + a_3V(0)^\beta} < \frac{1}{a_1a_2a_3(\beta-1)}. \quad (16)$$

□

Remark 5: Note that for the fixed-time stability lemma given in lemma 3, by setting $a = a_1a_2^2$, $b = a_1a_3^2$, $c = 2\,a_1a_2a_3$, $\rho_1 = \beta$ and $\rho_2 = 2 - \beta$, it is seen that lemma 4 can be written in the same form as given in lemma 3. This implies that lemma 4 is also a generalization of the previous popular fixed-time stability lemma.

Remark 6: The system of equations $\{a = a_1a_2^2, b = a_1a_3^2, c = 2\,a_1a_2a_3\}$ actually has infinitely many solutions. For $c = b^{\frac{3}{2}}\sqrt{a}$, to obtain the setting time T_s given by (8) for a given Lyapunov inequality written in the form of (5), one may set the value of a_3 arbitrarily to ease this particular process. In other words, setting $a_3 = \frac{p_1}{p_2}$ for some $p_1, p_2 > 0$, yields:

$$a_1 = \frac{b\,p_2^2}{p_1^2}, \quad a_2 = \sqrt{\frac{a}{b}}\frac{p_1}{p_2}, \quad a_3 = \frac{p_1}{p_2}. \quad (17)$$

To demonstrate that the given settling time in (8) is indeed less than that given by (6), we simply apply (6) with the parameters $\rho_1 = \beta$ and $\rho_2 = 2 - \beta$, $a = a_1a_2$, $b = a_1a_3$ and $c = 2\,a_1a_3$:

$$T_s^* = \frac{1}{2a_1a_2a_3(\beta-1)}\ln(1 + 2\,a_3)$$
$$+ \frac{1}{2a_1a_2a_3(\beta-1)}\ln(1 + 2\,a_2)$$
$$= \frac{1}{2a_1a_2a_3(\beta-1)}\ln(1 + 2\,a_3)(1 + 2a_2)$$

$$\geq \frac{1}{2a_1a_2a_3(\beta-1)}\ln(6)$$

$$\geq \frac{1}{2a_1a_2a_3(\beta-1)}\ln(e) \geq T_s. \tag{18}$$

It should be noted that since β is between 1 and 2, it thereby follows that the settling time in (8) is also less than the one presented in [45]. Hence, the boundary of our proposed convergence time is even more precise than the previous popular fixed-time stability lemmas. Furthermore, the expression for estimating this convergence time is simpler to compute compared to those provided in the previously popular fixed-time stability lemmas.

III. FIXED-TIME ADAPTIVE NONSINGULAR TERMINAL SLIDING MODE SYNCHRONIZATION OF A SEVEN-TERM HYPERCHAOTIC SYSTEM

In this section, we discuss the design of the fixed-time adaptive nonsingular terminal sliding mode controller for the synchronization of the 4D hyperchaotic system.

The dynamics of the six-term chaotic system presented in [26] are given as follows:

$$\dot{x}_1 = ax_1 + x_2x_3,$$
$$\dot{x}_2 = x_1 - x_2,$$
$$\dot{x}_3 = 1 - x_1^2. \tag{19}$$

By inserting an x_4 feedback term into the first equation of (19), and writing a dynamics equation for x_4, a 4-dimensional system can be obtained. The dynamic equations of the system are described by:

$$\dot{x}_1 = ax_1 + x_2x_3 + x_4,$$
$$\dot{x}_2 = x_1 - x_2,$$
$$\dot{x}_3 = 1 - x_1^2,$$
$$\dot{x}_4 = x_1x_3 - bx_4. \tag{20}$$

where the variables a and b are the system's parameters. Due to our primary focus on the control design and its circuit implementation, we defer the formal dynamical analysis of this particular system to our next scientific report.

A. CONTROL DESIGN

The primary goal of an active synchronization problem is to achieve synchronization between a chaotic system, referred to as the slave system, and an original chaotic system known as the master system [47]. Here, the master system is the original system of (19), rewritten here for convenience:

$$\dot{x}_{m,1} = ax_{m,1} + x_{m,2}x_{m,3} + x_{m,4},$$
$$\dot{x}_{m,2} = x_{m,1} - x_{m,2},$$
$$\dot{x}_{m,3} = 1 - x_{m,1}^2,$$
$$\dot{x}_{m,4} = x_{m,1}x_{m,3} - bx_{m,4}. \tag{21}$$

The slave system includes both the controller to be designed and the disturbance, and is given by:

$$\dot{x}_{s,1} = ax_{s,1} + x_{s,2}x_{s,3} + x_{s,4} + u_1 + d_1,$$

$$\dot{x}_{s,2} = x_{s,1} - x_{s,2} + u_2 + d_2,$$
$$\dot{x}_{s,3} = 1 - x_{s,1}^2 + u_3 + d_3,$$
$$\dot{x}_{s,4} = x_{s,1}x_{s,3} - bx_{s,4} + u_4 + d_4. \tag{22}$$

For the active synchronization problem, define the error states as $e_i = x_{s,i} - x_{m,i}$ where $i = 1, 2, 3, 4$. The error dynamics are given by:

$$\dot{e}_1 = ae_1 + x_{s,2}x_{s,3} - x_{m,2}x_{m,3} + e_4 + d_1 + u_1,$$
$$\dot{e}_2 = e_1 - e_2 + d_2 + u_2,$$
$$\dot{e}_3 = x_{s,1}^2 - x_{m,1}^2 + d_3 + u_3,$$
$$\dot{e}_4 = x_{s,1}x_{s,3} - x_{m,1}x_{m,3} - be_4 + d_4 + u_4. \tag{23}$$

Assumption 7: The disturbances are bounded, that is, there exist some constants $\delta_i > 0$, such that $|d_i| < \delta_i$.

The error system in (23) facilitates the design of an integral nonsingular terminal sliding mode control. For each error state $e_1 - e_4$, design now the integral terminal fast sliding surface as:

$$s_i = e_i + k_i \int_0^t \text{sig}(e_i)^{\eta_i} dt. \tag{24}$$

where $k_i > 0$ is the sliding surface gain. The parameters η_i are chosen to be fractions of odd numbers in a similar fashion to [48]. Note also that the sig function, defined in [48] and [49], is a lot more challenging to implement electronically. To allow for smooth circuit implementation of the sig function in the control design, the **sigr** function introduced in [26] and [50] is used to implement the sliding surface of (24). The modified integral terminal fast sliding surface is now rewritten as:

$$s_i = e_i + k_i \int_0^t \text{sigr}(e_i)^{\eta_i} dt. \tag{25}$$

The control signals $u_1(t) - u_4(t)$ may now be designed based on the integral terminal fast sliding surface (25). For the first error state e_1, the time derivative of the sliding surface s_1 is:

$$\dot{s}_1 = \dot{e}_1 + k_1 \text{sigr}(e_1)^{\eta_1}$$
$$= ae_1 + x_{s,2}x_{s,3} - x_{m,2}x_{m,3} + d_1 + u_1 + k_1\text{sigr}(e_1)^{\eta_1}. \tag{26}$$

Note that we now design u_1 as:

$$u_1 = -ae_1 - e_4 - x_{s,2}x_{s,3} + x_{m,2}x_{m,3} - k_1\text{sigr}(e_1)^{\eta_1}$$
$$- D_1\text{sigr}(s_1) - k_{s_1}s_1^{\eta_1}. \tag{27}$$

Note that the disturbance d_1 was not brought into the design of u_1. To account for the disturbance and other uncertainties and to eliminate the process of having to compute the uncertainties' upper bound, the following adaptive law is used to adjust the D_1 parameter:

$$\dot{D}_1 = \begin{cases} m_1|s_1|\text{signr}(s - \sigma_1), & \text{if } D_1 \geq \sigma_1 \\ \sigma_1 - m_2|s_1| - p_1D_1, & \text{if } D_1 < \sigma_1 \end{cases} \tag{28}$$

where σ_1 denotes some arbitrary threshold value that is assumed to be less than the disturbance upper bound δ_1. For

the second state error e_2, the time derivative of the sliding surface s_2 is:

$$\dot{s}_2 = \dot{e}_2 + k_2\text{sigr}(e_2)^{\eta_2}$$
$$= e_1 - e_2 + d_2 + u_2 + k_2\text{sigr}(e_2)^{\eta_2}. \quad (29)$$

The control signal u_2 is easily designed as:

$$u_2 = -e_1 + e_2 - k_2\text{sigr}(e_2)^{\eta_2} - D_2\text{sigr}(s_2) - k_{s_2}s_2^{\eta_2}. \quad (30)$$

In similar fashion to the design of D_1, the D_2 parameter is adjusted through the adaptive law:

$$\dot{D}_2 = \begin{cases} m_2|s_2|\text{signr}(s_2 - \sigma_2), & \text{if } D_2 \geq \sigma_2 \\ \sigma_2 - m_2|s_2| - p_2D_2, & \text{if } D_2 < \sigma_2 \end{cases} \quad (31)$$

where σ_2 is again the arbitrary threshold value, which is again less than the upper bound δ_2. The time derivative for the sliding surface s_3, corresponding to the state error e_3, is:

$$\dot{s}_3 = \dot{e}_3 + k_3\text{sigr}(e_3)^{\eta_3}$$
$$= e_1(x_{s,1} + x_{m,1}) + d_3 + u_3 + k_3\text{sigr}(e_3)^{\eta_3}. \quad (32)$$

The control signal u_3 is now designed as:

$$u_3 = -e_1(x_{m,1} + x_{s,1}) - k_3\text{sigr}(e_3)^{\eta_3} - D_3\text{sigr}(s_3) - k_{s_3}s_3^{\eta_3}. \quad (33)$$

The adaptive law for the adjustment of the D_3 parameter is given by:

$$\dot{D}_3 = \begin{cases} m_3|s_3|\text{signr}(s_3 - \sigma_3), & \text{if } D_3 \geq \sigma_3 \\ \sigma_3 - m_3|s_3| - p_3D_3, & \text{if } D_3 < \sigma_3 \end{cases}. \quad (34)$$

where σ_3 denotes the arbitrary threshold, assumed to be less than δ_3. Lastly, the time derivative for the sliding surface s_4 is now written thus:

$$\dot{s}_4 = \dot{e}_4 + k_4\text{sigr}(e_4)^{\eta_4}$$
$$= -be_4 + x_{s,1}x_{s,3} - x_{m,1}x_{m,3} + d_4 + u_4 + k_4\text{sigr}(e_4)^{\eta_4}. \quad (35)$$

The control signal u_4 is designed thus:

$$u_4 = be_4 - x_{s,1}x_{s,3} + x_{m,1}x_{m,3} - k_4\text{sigr}(e_4)^{\eta_4}$$
$$- D_4\text{sigr}(s_4) - k_{s_4}s_4^{\eta_4}, \quad (36)$$

where the adaptive law for the parameter D_4 is:

$$\dot{D}_4 = \begin{cases} m_4|s_4|\text{signr}(s_4 - \sigma_4), & \text{if } D_4 \geq \sigma_4 \\ \sigma_4 - m_4|s_4| - p_4D_4, & \text{if } D_4 < \sigma_4. \end{cases} \quad (37)$$

In (37), σ_4 is the arbitrary threshold, which is again considered to be less than the upper bound δ_4.

Remark 8: Note that this new controller is designed with the goal of ensuring easy electronics implementation and simplifying the design from [26]. Additionally, it incorporates disturbance rejection, a feature not included in [26].

B. FIXED-TIME STABILITY ANALYSES

Here we present the stability analyses for the fixed-time stability of the proposed controller. We then furnish the following theorem.

Theorem 9: Consider the error system (23) with the control signals u_1 designed by (27)-(28), u_2 as designed in (30)-(31), u_3 as designed in (33)-(34), and u_4 given by (36)-(37). Suppose also that the upper bound of the disturbance estimation is such that $|D_i^* - D_i| < \delta_i$, where D_i^* represents the actual disturbance. The error trajectories can be made to converge to zero in a fixed time. The estimated settling time is:

$$T_s = \max(T_{s_1}, T_{s_2}, T_{s_3}, T_{s_4}), \quad (38)$$

where

$$T_{s_i} = \frac{2^{\frac{3}{2}}}{\sqrt{\delta_i k_{s_i}}} \frac{1}{\eta_i - 1}. \quad (39)$$

Proof: We consider two cases, namely $s_i > \sigma_i$ and $s_i < \sigma_i$.

Case 1: $s_i > \sigma_i$. In this respect, we first prove the stability of the closed-loop error systems. For each error system, define the following Lyapunov candidate:

$$V_i = \frac{1}{2}s_i^2 + \frac{\xi_i}{2}(D_i^* - D_i)^2. \quad (40)$$

Its time differentiation yields:

$$\dot{V}_i = s_i\dot{s}_i + \xi_i(D_i^* - D_i)\dot{D}_i. \quad (41)$$

Substituting the control signal u_i, and the adaptive law $\dot{D}_i$ given in (28), (31), (34), (37) into (41) for the case where $s_i > \sigma_i$ gives:

$$\dot{V}_i = s_i(-D_i\text{sigr}(s_i) - k_{s_i}s_i^{\eta_i})$$
$$- \xi_i(D_i^* - D_i)[m_i|s_i|\text{signr}(s_i - \sigma_i)]. \quad (42)$$

It is obvious that as $s_i > \sigma_i$, the time differential of the Lyapunov candidate $\dot{V}_i \leq 0$. In applying Babalat's lemma, we note that (42) can be written as:

$$\dot{V}_i \leq \max(\xi_i, \delta_i, m_i)k_{s_i}2^{\frac{\eta_i+1}{2}}V^{\frac{\eta_i+1}{2}}. \quad (43)$$

Integrating, (43) then gives

$$V_i \leq \left[V(0)^{\frac{1-\eta_i}{2}} - \max(\xi_i, \delta_i, m_i)k_{s_i}2^{\frac{\eta_i+1}{2}}t\left(\frac{1-\eta_i}{2}\right)\right]^{\frac{2}{1-\eta_i}},$$

which implies that $\int_0^t V_i(\tau)\, d\tau$ is finite. Thus $V \to 0$ as $t \to \infty$, implying that $s \to 0$ as $t \to \infty$, which implies the global stability of the closed-loop system.

To prove the fixed-time stability, we note that (44) can be obtained by applying Young's inequality to (42):

$$\dot{V}_i \leq -\delta_i|s_i| - k_{s_i}s_i^{\eta_i+1} - m_i\xi_i(D_i^* - D_i)|s_i|$$
$$\leq -\delta_i|s_i| - k_{s_i}s_i^{\eta_i+1} - m_i\xi_i\left[\frac{1}{2}s_i^2 + \frac{1}{2}(D_i^* - D_i)^2\right]$$
$$\leq -\delta_i 2^{\frac{1}{2}}V^{\frac{1}{2}} - k_{s_i}2^{\frac{\eta_i+1}{2}}V^{\frac{\eta_i+1}{2}} - \xi_i m_i V. \quad (44)$$

Applying lemma 4 with $a = \delta_i 2^{\frac{1}{2}}$, $b = k_{s_i} 2^{\frac{\eta_i + 1}{2}}$ and $c = m_i \xi_i$, along with (17) and simplifying, yields the estimation of the settling time for the i-th sliding surface as:

$$T_{s_{Mi}} = \sqrt{\frac{2}{\delta_i k_{s_i}}} \left[\frac{1}{(\eta - 1)} \right].$$

Case 2: $s_i < \sigma_i$. Consider again the Lyapunov candidate of (40) with its time differentiation given by (41). When $s_i < \sigma_i$, the second adaptive law for $\dot{D}$ is invoked. Substituting the control law u_i, and the second adaptive law for $\dot{D}_i$, we have:

$$\dot{V}_i = s_i(-D_i \text{signr}(s_i) - k_{s_i} s_i^{\eta_i})$$
$$- \xi_i(D_i^* - D_i)(\sigma_i - m_i|s_i| - p_i D_i),$$
$$\leq -\delta_i|s_i| - k_{s_i} s_i^{\eta_i + 1}$$
$$+ \xi_i(D_i^* - D_i)((1 + p_i)\sigma_i - m_i|s_i|). \quad (45)$$

As $s_i < \sigma_i$, the second adaptive law then brings the time differential of the Lyapunov candidate back to $\dot{V}_i \leq 0$, so that the global stability for the closed loop system is again proven. To prove the fixed-time stability for this case, applying Young's inequality to (45), we obtain:

$$\dot{V}_i \leq -\delta_i|s_i| - k_{s_i} s_i^{\eta_i + 1} + \xi_i(D_i^* - D_i)((1 + \rho_i)\sigma_i - m_i|s_i|)$$
$$\leq -\delta_i|s_i| - k_{s_i} s_i^{\eta_i + 1} - (2m_2 - (1 + \rho_i)\sigma_i)\xi_i$$
$$\cdot \left[\frac{1}{2} s_i^2 + \frac{1}{2}(D_i^* - D_i)^2 \right]$$
$$\leq -\delta_i 2^{\frac{1}{2}} V^{\frac{1}{2}} - k_{s_i} 2^{\frac{\eta_i + 1}{2}} V^{\frac{\eta_i + 1}{2}} - (2m_2 - (1 + p_i)\sigma_i)\xi_i V. \quad (46)$$

Applying lemma 4 with $a = \delta_i 2^{\frac{1}{2}}$, $b = k_{s_i} 2^{\frac{\eta_i + 1}{2}}$ and $c = [2m_2 - (1 + \rho_i)\sigma_i]\xi_i$, along with (17) and simplifying gives the settling time estimation to be:

$$T_{sL_i} = \frac{2^{\frac{1}{2}}}{\sqrt{\delta_i k_{s_i}}} \left[\frac{1}{\eta_i - 1} \right]. \quad (47)$$

The total settling time is now given by:

$$T_{s_i} = T_{s_{Mi}} + T_{sL_i}$$
$$= \frac{2^{\frac{3}{2}}}{\sqrt{\delta_i k_{s_i}}} \left[\frac{1}{\eta_i - 1} \right]. \quad (48)$$

Taking the maximum of all the settling times gives the total estimate of the reach time. $\square$

Remark 10: In many practical engineering systems, it is reasonable to assume that the disturbances are bounded, so that Assumption 7 is reasonable. In previous works, the disturbances were taken care of by inserting the term $\delta_i \text{sign}(e_i)$ into the controller u_i, which did not force the disturbance itself to converge to zero. However, the proof of Theorem 9 analyzes the effects of the adaptive gain rule to ensure that the overall closed-loop system can be stabilized in fixed time, even in the effect of disturbances.

Remark 11: Note that the value of the settling time T_s given in (39) is influenced mainly by the control gain

parameter k_{s_i} and the power parameter η_i, therefore, choosing a larger value for these parameters would result in a lower T_s. However, the k_{s_i} is also the multiplier of the signr function; thus, the main cost of choosing a larger k_{s_i} is the increment of the chattering. A good guideline therefore is to tune all the control parameters using a metaheuristic optimization algorithm with the constraint $k_{s_i} \in (0.1, 5)$.

C. COMPUTER SIMULATION RESULTS

In the computer simulations of the proposed controller, we assign the system parameters as $a = -0.042$ and $b = -0.06$. The initial conditions of the master system x_{m0} are taken to be:

$$x_{m0} = [5, 1.1, 0.5, -0.06]. \quad (49)$$

The initial states of the slave system is given by:

$$x_{s0} = [1.1, -1.1, 0.1, 0.1]. \quad (50)$$

Notably, due to the lack of space, our focus will be on the case where the disturbances are set in a chaotic system. The disturbance functions are:

$$d_1 = 0.05 \sin(1.4\,t), \quad d_2 = 0.2 \sin(1.6\,t), \quad (51)$$
$$d_3 = 0.3 \sin(1.6\,t), \quad d_4 = 0.5 \sin(1.6\,t). \quad (52)$$

The control parameters are tuned using the extended exploration grey wolf optimization presented in [50] and [51] with the constraint of $k_{s_i} \in (0.1, 5)$ and are given by:

$$k_1 = 2, \quad k_2 = 5, \quad k_3 = 8, \quad k_4 = 6, \quad (53)$$
$$k_{s1} = 0.7, \quad k_{s2} = 0.5, k_3 = 2.0, \quad k_{s4} = 0.002, \quad (54)$$
$$p_1 = 0.1, \quad p_2 = 0.005, \quad p_3 = 0.005, \quad p_4 = 0.005, \quad (55)$$
$$m_1 = 0.5, \quad m_2 = 0.5, \quad m_3 = 0.6, \quad m_4 = 0.8, \quad (56)$$
$$\eta_1 = 1.025, \quad \eta_2 = 1.025, \quad \eta_3 = 1.025, \quad \eta_4 = 1.025. \quad (57)$$

Fig. 1 now depicts the phase portraits for the synchronization between the $(x_1(t), x_2(t))$ and $(x_3(t), x_4(t))$ states. Fig. 2 shows the synchronization errors e_1, e_2, e_3, and e_4. As seen, the active synchronization is achieved within about 1 second, which is of course faster than those reported in previous works [18], [52]. The control efforts u_1 - u_4 are plotted in Fig. 3. Note that higher k_i values could, of course, be used, but the resulting control signals would be excessively high and constrained by the supply rails, thereby elongating the convergence times. The control efforts used in our design are about 30, which electronically means that for x_1 - x_4 signals in the order of mV, the main control signals would just be around 300 mV, which is well within the supply rails for the IC of 12V-15 V. Note also that our previous design through the nonterminal integral backstepping sliding mode control [26] had a maximal control effort of approximately 1200, which is significantly higher than our design, thereby expending more energy.
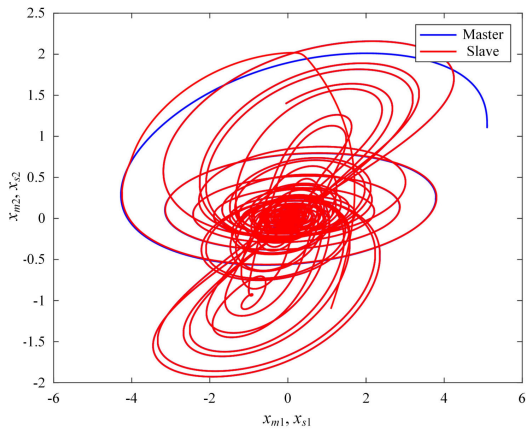
(a) Phase portrait for the synchronization of the (x_1, x_2) states
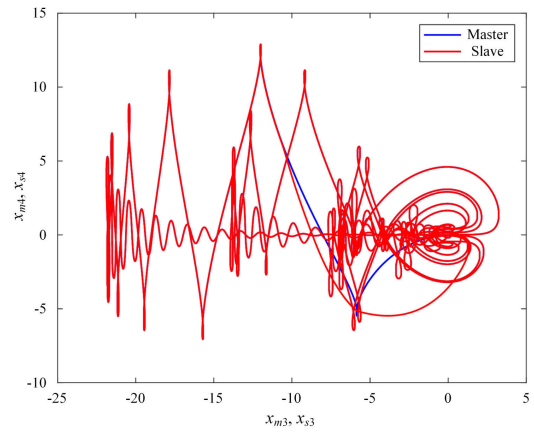
(b) Phase portrait for the synchronization of the (x_3, x_4) states

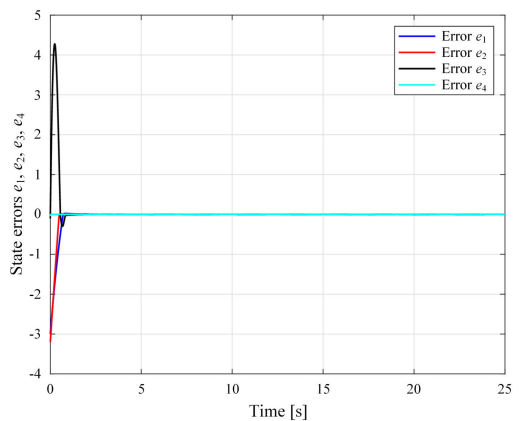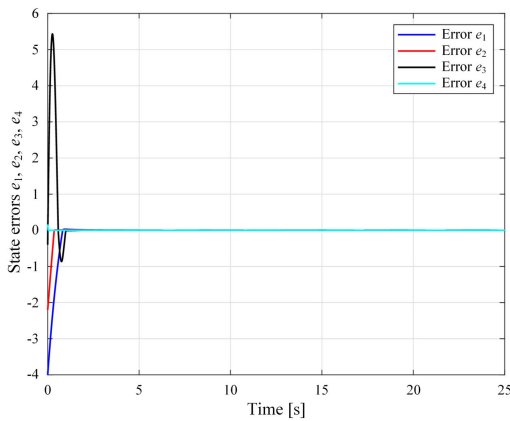**FIGURE 1. Synchronization between the master and slave signals.**

FIGURE 2. Synchronization errors e_1, e_2, e_3, e_4.

FIGURE 4. Synchronization errors e_1, e_2, e_3, e_4 for the initial condition given by (58).
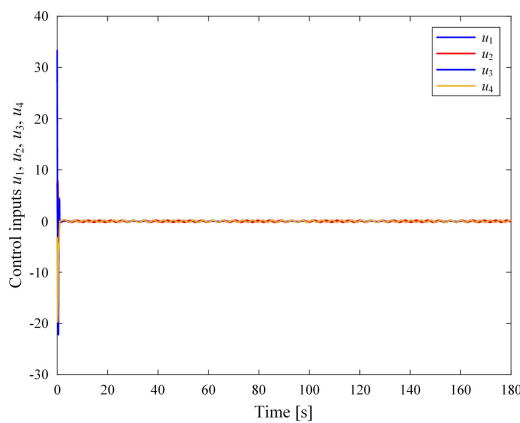

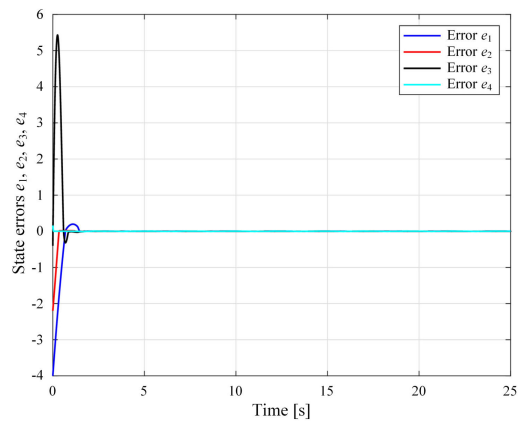**FIGURE 3. Control inputs u_1, u_2, u_3, u_4.**

FIGURE 5. Synchronization errors e_1, e_2, e_3, e_4 under 50% system and disturbance parameters uncertainties.

To explore how the initial conditions impact the uniformity of convergence time, the initial states of the slave system are altered to the following:

$$x_{s0} = [2.1, -2.1, 0.4, -0.1]. \qquad (58)$$

The disturbance functions are still given by (51)-(52). Fig. 4 shows the synchronization errors e_1, e_2, e_3 and e_4 for this particular case. It is easily seen from Fig. 4 that the trajectory
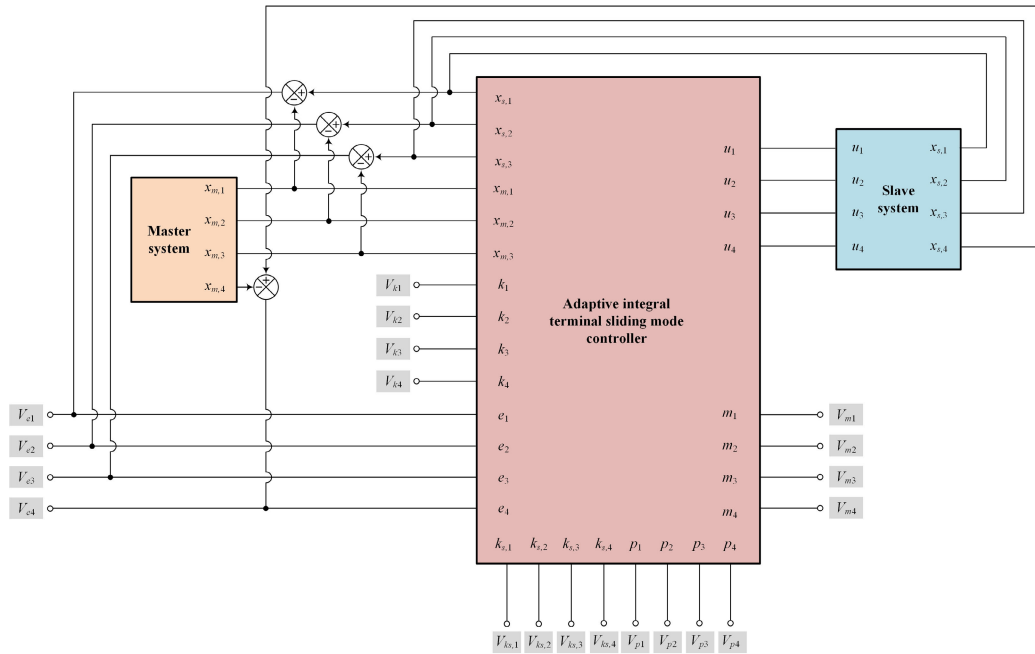
FIGURE 6. Overall schematic for the electronic circuit realization of the proposed seven-term hyperchaotic 4D system.
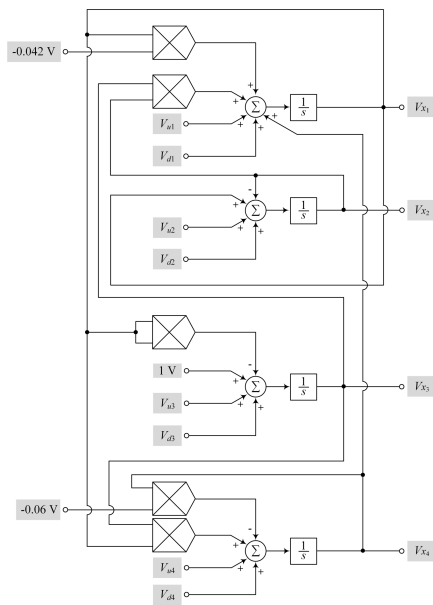

FIGURE 7. Circuit implementation of the master and slave systems for proposed hyperchaotic 4D system.

of the modified system converges to zero quickly, even though the initial conditions have significantly changed. Specifically, the convergence time for this case is also found to be around 1 second, which is similar to the case shown in Fig. 2. Thus, the numerical results obviously testify to the fixed-time feature of the developed control strategy.

An additional significant proof-of-concept concerns the synchronization of our chaotic system under parameter

errors and disturbance bounds uncertainties. In this light, we consider the case where the parameters a and b are set to -0.063 and -0.09, respectively, representing a 50% decrease. The disturbance functions are then given by:

$$d_{1,u}(t) = 0.75 \sin(2.1\,t), \quad d_{2,u}(t) = 0.3 \sin(2.4\,t), \quad (59)$$
$$d_{3,u}(t) = 0.45 \sin(2.4\,t), \quad d_{4,u}(t) = 0.75 \sin(2.4\,t). \quad (60)$$

Note that the amplitudes and frequencies of $d_{1,u}(t)$ - $d_{4,u}(t)$ are incremented by 50% from their original values in (51)-(52). These values provide significant bounds for the uncertainties in the system and disturbance parameters, which could actually take any values in between. The synchronization errors under these systems and disturbance parameters uncertainties are plotted in Fig. 5. As is seen, it can be concluded that no significant differences could be discerned between the results of Fig. 5 and Fig. 2, which was the case of the true value. These results imply that the designed adaptive terminal fixed-time sliding mode controller is definitely robust to extreme parameter and disturbance changes. This is definitely an advantage for the electronic implementation, where the designer does not have to set a precise value of a_{true} and b_{true} to obtain the exact results as in the ideal case.

IV. CIRCUIT REALIZATION OF THE CLOSED-LOOP SYSTEM
A. CIRCUIT DESIGN AND REALIZATION
In this section, we focus on the electronic circuit implementation of the closed-loop system for the proposed seven-term hyperchaotic 4D system. The overall design is shown in Fig. 6. The operational amplifier (OA) holds significant

(a) Integral terminal fixed-time sliding mode surface

(b) Control signal u_1

(c) Control signal u_2

(d) Control signal u_3
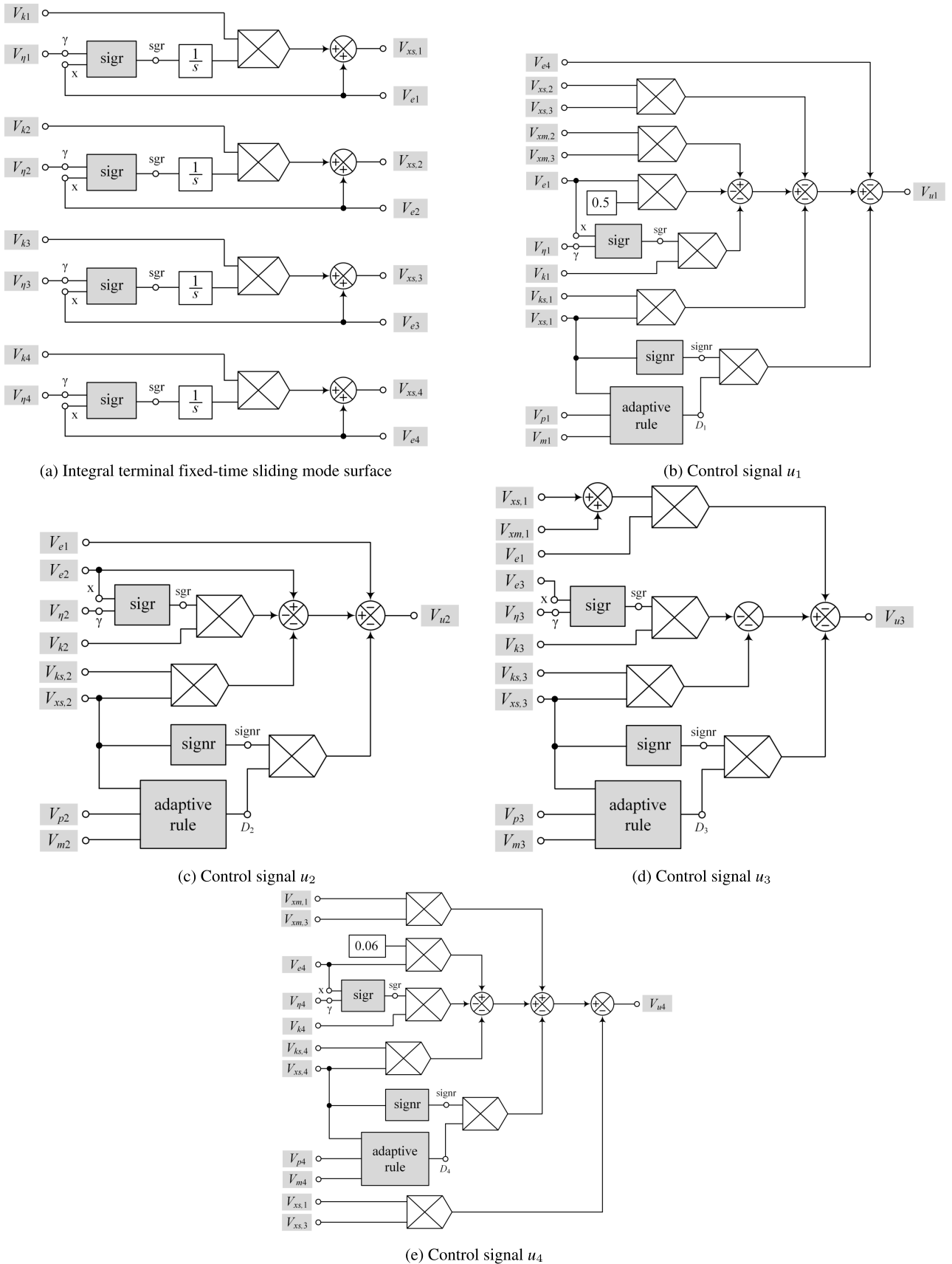
(e) Control signal u_4

FIGURE 8. Adaptive integral terminal sliding mode controller used in the proposed seven-term hyperchaotic 4D system.
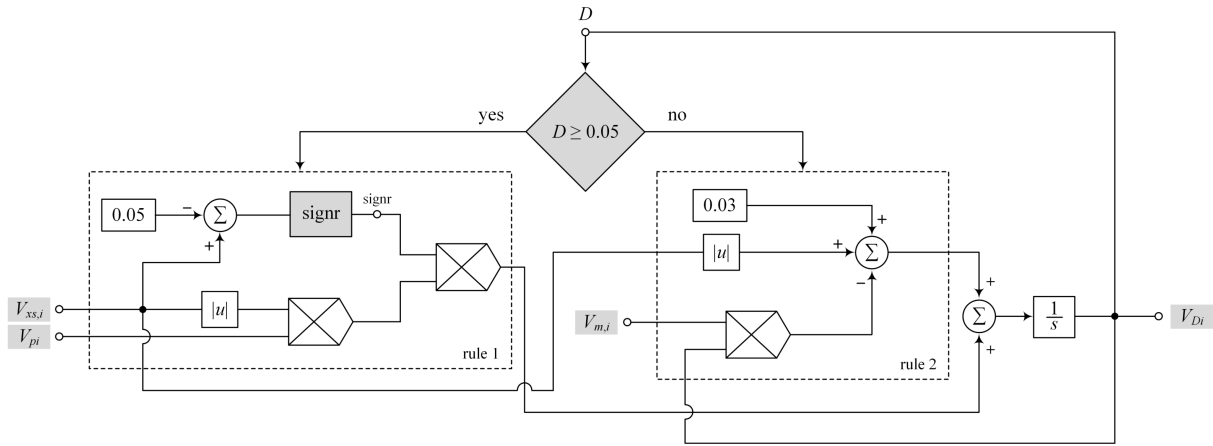
FIGURE 9. Adaptive rule used in adaptive integral terminal sliding mode controller.
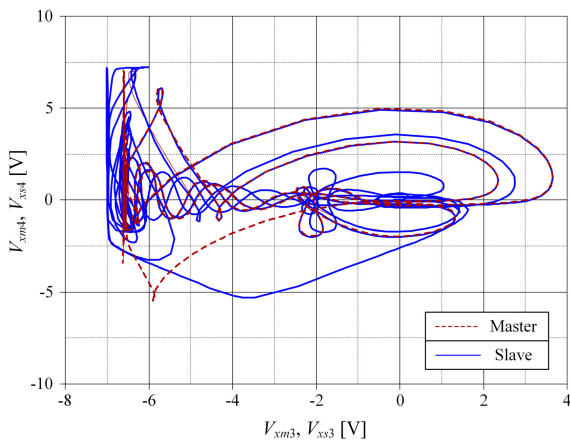

FIGURE 10. Circuit realization results for the synchronization between the master- and slave- systems.

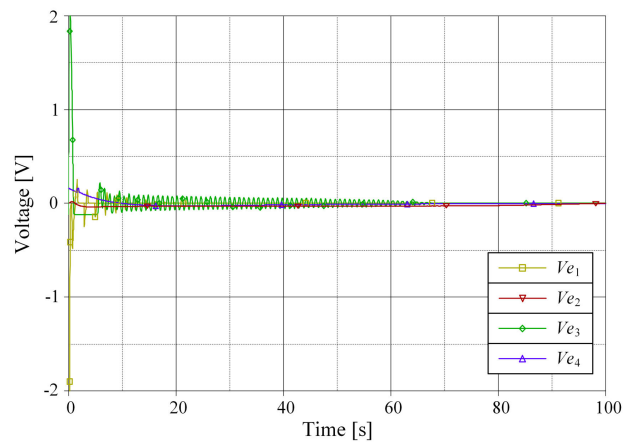**FIGURE 11.** The synchronization errors e_1, e_2, e_3, e_4 of the proposed system in Fig. 6 with disturbance parameters.

importance as a well-established electronic component in circuit design. Various circuit configurations utilizing reputable OA-based functions, such as integrators, differential amplifiers, and signal inverters, have been successfully implemented with actual physical circuitry [53]. Furthermore, the proposed system utilized not only the OA, but also the analog multiplier circuit described in [26]. The proposed closed-loop hyperchaotic 4D system is shown in Fig. 7, along with the analog circuits for both the master and slave systems. Moreover, the adaptive integral nonterminal sliding mode controller and its associated adaptive rules are implemented as shown in Figs. 8-9. By analyzing the proposed circuit with the terminal relationships of the OA, the master system for a seven-term chaotic 4D system in (21) can be rewritten in terms of the voltages as follows:

$$
\begin{aligned}
V_{\dot{x}_{m,1}} &= aV_{x_{m,1}} + V_{x_{m,2}}V_{x_{m,3}} + V_{x_{m,4}}, \\
V_{\dot{x}_{m,2}} &= V_{x_{m,1}} - V_{x_{m,2}}, \\
V_{\dot{x}_{m,3}} &= 1 - V_{x_{m,1}}^2, \\
V_{\dot{x}_{m,4}} &= V_{x_{m,1}}V_{x_{m,3}} - bV_{x_{m,4}},
\end{aligned}
\tag{61}
$$

$$
a = \frac{R_1}{R}, \tag{62}
$$

$$
b = \frac{R_2}{R}. \tag{63}
$$

It is noted from (62)-(63) that the values of the system parameters a and b can be tuned simply through resistors R_1 and R_2, respectively [26]. Likewise, the slave system, together with the controller and the disturbance, is also represented as:

$$
\begin{aligned}
V_{\dot{x}_{s,1}} &= aV_{x_{s,1}} + V_{x_{s,2}}V_{x_{s,3}} + V_{x_{s,4}} + V_{u_1} + V_{d_1}, \\
V_{\dot{x}_{s,2}} &= V_{x_{s,1}} - V_{x_{s,2}} + V_{u_2} + V_{d_2}, \\
V_{\dot{x}_{s,3}} &= 1 - V_{x_{s,1}}^2 + V_{u_3} + V_{d_3}, \\
V_{\dot{x}_{s,4}} &= V_{x_{s,1}}V_{x_{s,3}} - bV_{x_{s,4}} + V_{u_4} + V_{d_4}.
\end{aligned}
\tag{64}
$$

The state errors for the synchronization of the master and slave systems are computed as:

$$
\begin{aligned}
V_{\dot{e}_1} &= aV_{e_1} + V_{x_{s,2}}V_{x_{s,3}} - V_{x_{m,2}}V_{x_{m,3}} + V_{e_4} + V_{d_1} + V_{u_1}, \\
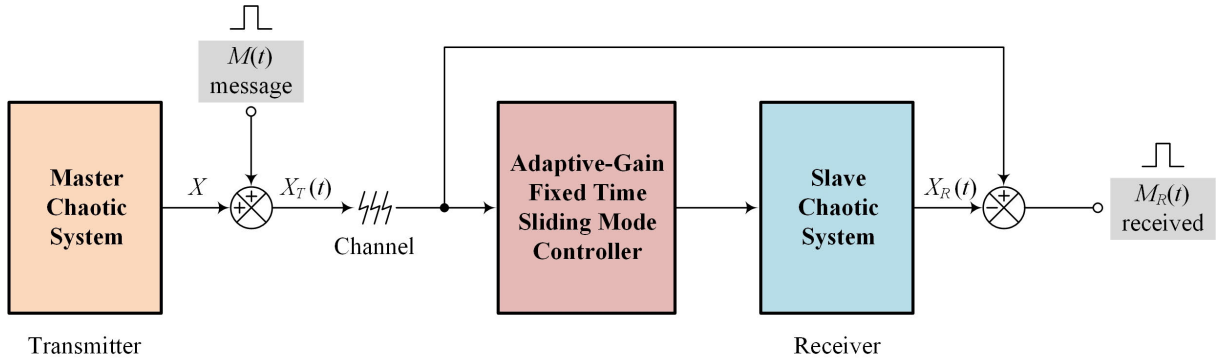V_{\dot{e}_2} &= V_{e_1} - V_{e_2} + V_{d_2} + V_{u_2},
\end{aligned}
$$

FIGURE 12. Block diagram schematic for the secure communication application.

$$V_{\dot{e}_3} = V_{x_{s,1}}^2 - V_{x_{m,1}}^2 + V_{d_3} + V_{u_3},$$

$$V_{\dot{e}_4} = V_{x_{s,1}}V_{x_{s,3}} - V_{x_{m,1}}V_{x_{m,3}} - bV_{e_4} + V_{d_4} + V_{u_4}, \quad (65)$$

where $V_{e_i} = V_{x_{s,i}} - V_{x_{m,i}}$. To implement the control signal designed in (27), (30), (33), and (36) based on the analog circuitry, we first implement the terminal fast sliding surface by:

$$V_{s_i} = V_{e_i} + V_{k_i} \int_0^t \mathrm{sigr}(V_{e_i})^{\eta_i} dt, \quad (66)$$

then the control signal parameters can be rewritten as:

$$V_{u_1} = -aV_{e1} - V_{e4} - V_{x_{s,2}}V_{x_{s,3}} + V_{x_{m,2}}V_{x_{m,3}}$$
$$- V_{k1}\mathrm{sigr}(V_{e1})^{\eta_1} - V_{D1}\mathrm{sigr}(V_{s1}) - V_{k_{s,1}}V_{s1}^{\eta_1}, \quad (67)$$

$$V_{u_2} = -V_{e1} + V_{e2} - V_{k2}\mathrm{sigr}(V_{e2})^{\eta_2} - V_{D2}\mathrm{sigr}(V_{s2})$$
$$- V_{k_{s,2}}V_{s2}^{\eta_2}, \quad (68)$$

$$V_{u_3} = -V_{e1}(V_{x_{m,1}} + V_{x_{s,1}}) - V_{k3}\mathrm{sigr}(V_{e3})^{\eta_3}$$
$$- V_{D3}\mathrm{sigr}(V_{s3}) - V_{k_{s,3}}V_{s3}^{\eta_3}, \quad (69)$$

$$V_{u_4} = bV_{e4} - V_{x_{s,1}}V_{x_{s,3}} + V_{x_{m,1}}V_{x_{m,3}}$$
$$- V_{k4}\mathrm{sigr}(V_{e4})^{\eta_4} - V_{D4}\mathrm{sigr}(V_{s4}) - V_{k_{s,4}}V_{s4}^{\eta_4}. \quad (70)$$

Note that the electronic implementation of the sigr function was presented previously in [50], thereby alleviating the chattering that resulted from the terminal fast sliding mode surface.

B. PSPICE ELECTRONICS WORKABILITY TEST

As a further demonstration of the concept, the PSPICE program is employed to simulate the comparison of the master and slave systems for the proposed hyperchaotic 4D system, which is based on the off-the-shelf IC OA LF357 macro-model provided by National Semiconductor [54] and the analog multiplier AD633 macro-model provided by Analog Devices [55], as illustrated in Fig. 7. In the simulation, the supply voltages are applied at ± 10 V. The system parameters a and b are set as -0.042 and -0.06, respectively, in order to generate either chaotic flows or stable equilibria. The initial states of the master system ($V_{x_{m,0}}$) and slave system ($V_{x_{s,0}}$) are set to be: $V_{x_{m,0}} = [5, 1.1, 0.5, -0.06]$ V and $V_{x_{s,0}} = [1.1, -1.1, 0.1, 0.1]$ V, in accordance with the
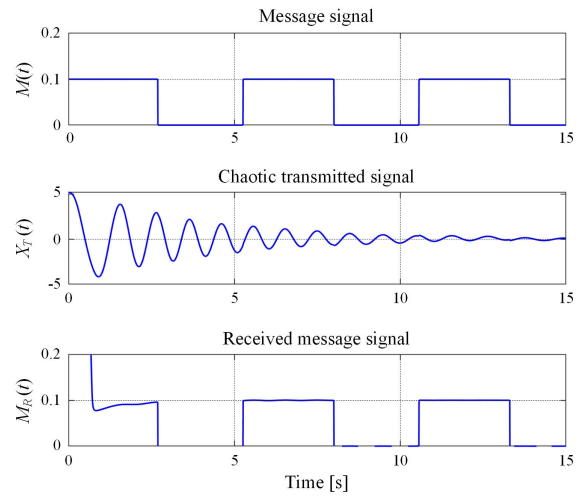

FIGURE 13. The original, chaotic masked, and recovered message signals for the secure communication application.

Matlab simulation. The disturbance functions of (51)-(52) were applied to the chaotic system as: $V_{d_1} = 0.05\sin(1.4\,t)$ V, $V_{d_2} = 0.2\sin(1.6\,t)$ V, $V_{d_3} = 0.3\sin(1.6\,t)$ V, and $V_{d_4} = 0.5\sin(1.6\,t)$ V. Furthermore, the control parameters offered in (53)-(57) are applied in terms of voltage to the proposed controller in Figs. 8-9. Depending on the provided parameters, the simulation results of the synchronization between the master system ($V_{x_{m,3}}$, $V_{x_{m,4}}$) and the slave system ($V_{x_{s,3}}$, $V_{x_{s,4}}$) are presented in Fig. 10. Fig. 11 shows the synchronization errors e_1, e_2, e_3, and e_4 of the proposed system in Fig. 6 with disturbance parameters. Attributable to the OA slew rates, the synchronization time of all error signals V_{e1}, V_{e2}, V_{e3}, and V_{e4} approached 0 V within 70 seconds with offset voltages of 0.462 mV, -8.999 mV, 0.203 mV, and -1.923 mV, respectively. Note that although we have used the macro model that was tried and tested by the manufacturer in the SPICE simulations, which would already be close enough to the actual circuit realization, these models may still not reflect fully the reality of the realization. Numerous factors, such as component tolerances, non-idealities, and so forth, would still have to be considered, which may also affect the setting time performance of the control. To enhance these

response capabilities, controllers could be implemented with high-performance active elements possessing a higher slew rate.

V. APPLICATION TO SECURE COMMUNICATION

The main features of a chaotic system, namely sensitivity to initial conditions, unpredictability, and anti-interception capability, make it challenging to produce and predict, and therefore ideal for applications in secure communications. Three main types of chaotic secure communication exist, namely chaotic masking, chaotic modulation, and chaotic shift keying [37]. Chaotic Masking is preferred in this work due to the fact that it does not require high channel signal-to-noise ratio (SNR). The variable $M(t)$ is the message signal, $X_T(t)$ is the transmitted signal, $X_R(t)$ is the synchronized chaotic signal, and $M_R(t)$ is the received message signal. Note that since identical chaotic systems are employed for both the transmitter and receiver sides, the chaotic signal from the receiver side is synchronized with the transmitter side. For synchronization, the initial conditions of (49) and (50) are used for the master and slave systems of the 4D chaotic system. Note that the control parameters of (53)-(57) are used for the secure communication system. Fig. 12 shows the schematic of secure communication using the 4D chaotic system.

For the numerical simulation, the message signal $M(t)$ is taken to be a pulse signal with an amplitude of 0.1 V, which is around 25 dB weaker than the chaotic signal. It is then seen from Fig. 13 that, after a fixed-time transient state of around 1 s, the original and recovered messages are nearly identical to one another, thereby implying that the 4D chaotic system, when combined with its fixed-time adaptive gain nonsingular terminal sliding mode controller, can be efficiently applied in secure communication applications.

VI. CONCLUSION

In this work, an adaptive gain fixed-time nonsingular terminal integral sliding mode control controller was designed with a view to simplifying a closed-loop electronic implementation of active synchronization of chaotic systems, as well as achieving convergence in fixed-time. The overall control design starts with designing a novel fixed-time stability lemma, which was theoretically demonstrated to provide a lower convergence estimate of the settling time than the previous popular stability notions, as well as being simpler mathematically to compute. A seven-term hyperchaotic system was presented, and a nonsingular terminal integral sliding mode controller was then designed to actively synchronize the system. An adaptive gain law was also incorporated into the controller to facilitate disturbance rejection. A theoretical proof was subsequently presented, demonstrating that synchronization was achieved within a fixed time. Simulation results confirm that synchronization was indeed achieved at a fixed time in the presence of disturbances. As further proof-of-concept, the parameters of the system as well as the disturbances were significantly

altered. Results show that the designed controller was robust to these changes, whilst still achieving the fixed-time control. An application to secure communication was also presented, whereby the developed controller is used to effectively synchronize the chaotic masked signal from the receiver side to the transmitter side. The outcomes demonstrate that the original and recovered messages are nearly identical to one another within a fixed time.

Finally, adaptive fixed-time active synchronization was realized through the use of commercially available active devices such as LF357 op-amps and AD633 analog multipliers. The descriptive circuit equations are formulated to emulate the control equations, aiming to simplify and facilitate troubleshooting. Workability of the electronic realizations was evaluated via PSPICE simulation program. Results show that the master and slave systems synchronized with a 1% maximal error, even under the effect of disturbances. Future research may highlight the development and implementation of the design using other electronically tunable active building blocks, such as transconductance amplifier-based active devices.

REFERENCES

[1] E. N. Lorenz, "Deterministic nonperiodic flow," *J. Atmos. Sci.*, vol. 20, no. 2, pp. 130–141, Mar. 1963.

[2] Y. Miladi, M. Feki, and N. Derbel, "Stabilizing the unstable periodic orbits of a hybrid chaotic system using optimal control," *Commun. Nonlinear Sci. Numer. Simul.*, vol. 20, no. 3, pp. 1043–1056, Mar. 2015.

[3] T. Matsumoto, "A chaotic attractor from Chua's circuit," *IEEE Trans. Circuits Syst.*, vol. CS-31, no. 12, pp. 1055–1058, Dec. 1984.

[4] S. Sampath, S. Vaidyanathan, C. K. Volos, and V. T. Pham, "An eight-term novel four-scroll chaotic system with cubic nonlinearity and its circuit simulation," *J. Eng. Sci. Technol. Rev.*, vol. 8, no. 2, pp. 1–6, 2015.

[5] V.-T. Pham, C. Volos, S. Jafari, Z. Wei, and X. Wang, "Constructing a novel no-equilibrium chaotic system," *Int. J. Bifurcation Chaos*, vol. 24, no. 5, May 2014, Art. no. 1450073.

[6] T. Gotthans, J. C. Sprott, and J. Petrzela, "Simple chaotic flow with circle and square equilibrium," *Int. J. Bifurcation Chaos*, vol. 26, no. 8, Jul. 2016, Art. no. 1650137.

[7] S. Jafari, J. C. Sprott, and M. Molaie, "A simple chaotic flow with a plane of equilibria," *Int. J. Bifurcation Chaos*, vol. 26, no. 6, Jun. 2016, Art. no. 1650098.

[8] J. O. Maaita, C. K. Volos, I. M. Kyprianidis, and I. N. Stouboulos, "The dynamics of a cubic nonlinear system with no equilibrium point," *J. Nonlinear Dyn.*, vol. 2015, pp. 1–13, Sep. 2015.

[9] M. T. Yassen, "Controlling chaos and synchronization for new chaotic system using linear feedback control," *Chaos, Solitons Fractals*, vol. 26, no. 3, pp. 913–920, Nov. 2005.

[10] F. Wang and C. Liu, "A new criterion for chaos and hyperchaos synchronization using linear feedback control," *Phys. Lett. A*, vol. 360, no. 2, pp. 274–278, Dec. 2006.

[11] S. Vaidyanathan, "Adaptive chaos control and synchronization of hyperchaotic LIU system," *Int. J. Comput. Sci., Eng. Inf. Technol.*, vol. 1, no. 2, pp. 29–40, Jun. 2011.

[12] S. Vaidyanathan, "Global chaos synchronization of the forced van der pol chaotic oscillators via adaptive control method," *Int. J. Pharmtech Res.*, vol. 8, no. 6, pp. 156–166, 2015.

[13] S. Vaidyanathan, "Anti-synchronization of novel coupled van der pol conservative chaotic systems via adaptive control method," *Int. J. Pharmtech Res.*, vol. 9, no. 2, pp. 106–123, 2016.

[14] A. El-Gohary, "Optimal synchronization of Rössler system with complete uncertain parameters," *Chaos Solit. Fractals*, vol. 27, no. 2, pp. 345–355, 2006.

[15] S. Rasappan and S. Vaidyanathan, "Hybrid synchronization of n–scroll Chua and Lur'e chaotic systems via backstepping control with novel feedback," *Arch. Control Sci.*, vol. 22, no. 3, pp. 255–278, 2012.

[16] H. Delavari and M. Mohadeszadeh, "Robust finite-time synchronization of non-identical fractional-order hyperchaotic systems and its application in secure communication," *IEEE/CAA J. Autom. Sinica*, vol. 6, no. 1, pp. 228–235, Jan. 2019.

[17] S. Rasappan and S. Vaidyanathan, "Global chaos synchronization of WINDMI and Coullet chaotic systems using adaptive backstepping control design," *Kyungpook Math. J.*, vol. 54, no. 2, pp. 293–320, Jun. 2014.

[18] S. Vaidyanathan, S. T. Kingni, A. Sambas, M. A. Mohamed, and M. Mamat, "A new chaotic jerk system with three nonlinearities and synchronization via adaptive backstepping control," *Int. J. Eng. Technol.*, vol. 7, no. 3, p. 1936, Aug. 2018.

[19] B. Vaseghi, M. A. Pourmina, and S. Mobayen, "Secure communication in wireless sensor networks based on chaos synchronization using adaptive sliding mode control," *Nonlinear Dyn.*, vol. 89, no. 3, pp. 1689–1704, Aug. 2017.

[20] I.-C. Baik, K.-H. Kim, and M.-J. Youn, "Robust nonlinear speed control of PM synchronous motor using boundary layer integral sliding mode control technique," *IEEE Trans. Control Syst. Technol.*, vol. 8, no. 1, pp. 47–54, Jan. 2000.

[21] U. E. Kocamaz, B. Cevher, and Y. Uyaroğlu, "Control and synchronization of chaos with sliding mode control based on cubic reaching rule," *Chaos, Solitons Fractals*, vol. 105, pp. 92–98, Dec. 2017.

[22] S. P. Bhat and D. S. Bernstein, "Finite-time stability of continuous autonomous systems," *SIAM J. Control Optim.*, vol. 38, no. 3, pp. 751–766, Jan. 2000.

[23] M. P. Aghababa and H. P. Aghababa, "Chaos suppression of uncertain gyros in a given finite time," *Chin. Phys. B*, vol. 21, no. 11, Nov. 2012, Art. no. 110505.

[24] J.-K. Ni, C.-X. Liu, K. Liu, and L. Liu, "Finite-time sliding mode synchronization of chaotic systems," *Chin. Phys. B*, vol. 23, no. 10, Oct. 2014, Art. no. 100504.

[25] H. Xue and X. Liu, "A novel fast terminal sliding mode with predefined-time synchronization," *Chaos, Solitons Fractals*, vol. 175, Oct. 2023, Art. no. 114049.

[26] N. Wongvanich, N. Roongmuanpha, and W. Tangsrirat, "Finite-time integral backstepping nonsingular terminal sliding mode control to synchronize a new six-term chaotic system and its circuit implementation," *IEEE Access*, vol. 11, pp. 22233–22249, 2023.

[27] A. Polyakov and L. Fridman, "Stability notions and Lyapunov functions for sliding mode control systems," *J. Franklin Inst.*, vol. 351, no. 4, pp. 1831–1865, Apr. 2014.

[28] C. Chen, L. Li, H. Peng, Y. Yang, L. Mi, and H. Zhao, "A new fixed-time stability theorem and its application to the fixed-time synchronization of neural networks," *Neural Netw.*, vol. 123, pp. 412–419, Mar. 2020.

[29] C. Hu, J. Yu, Z. Chen, H. Jiang, and T. Huang, "Fixed-time stability of dynamical systems and fixed-time synchronization of coupled discontinuous neural networks," *Neural Netw.*, vol. 89, pp. 74–83, May 2017.

[30] B. Tian, Z. Zuo, X. Yan, and H. Wang, "A fixed-time output feedback control scheme for double integrator systems," *Automatica*, vol. 80, pp. 17–24, Jun. 2017.

[31] B. Tian, H. Lu, Z. Zuo, and H. Wang, "Fixed-time stabilization of high-order integrator systems with mismatched disturbances," *Nonlinear Dyn.*, vol. 94, no. 4, pp. 2889–2899, Dec. 2018.

[32] J. Ni, C. K. Ahn, L. Liu, and C. Liu, "Prescribed performance fixed-time recurrent neural network control for uncertain nonlinear systems," *Neurocomputing*, vol. 363, pp. 351–365, Oct. 2019.

[33] A.-M. Zou and Z. Fan, "Fixed-time attitude tracking control for rigid spacecraft without angular velocity measurements," *IEEE Trans. Ind. Electron.*, vol. 67, no. 8, pp. 6795–6805, Aug. 2020.

[34] Y. Su, C. Zheng, and P. Mercorelli, "Robust approximate fixed-time tracking control for uncertain robot manipulators," *Mech. Syst. Signal Process.*, vol. 135, Jan. 2020, Art. no. 106379.

[35] C. Chen, L. Li, H. Peng, Y. Yang, L. Mi, and L. Wang, "A new fixed-time stability theorem and its application to the synchronization control of memristive neural networks," *Neurocomputing*, vol. 349, pp. 290–300, Jul. 2019.

[36] A. Khanzadeh, M. Pourgholi, and E. Amini Boroujeni, "A novel condition for fixed-time stability and its application in controller design for robust fixed-time chaos stabilization against Hölder continuous uncertainties," *Soft Comput.*, vol. 25, no. 5, pp. 3903–3911, Mar. 2021.

[37] K. Sun, *Chaotic Secure Communication*. Berlin, Germany: Walter de Gruyter, 2016.

[38] S. Cui and J. Zhang, "Chaotic secure communication based on single feedback phase modulation and channel transmission," *IEEE Photon. J.*, vol. 11, no. 5, pp. 1–8, Oct. 2019.

[39] D. M. Semenov and A. L. Fradkov, "Adaptive synchronization in the complex heterogeneous networks of Hindmarsh–Rose neurons," *Chaos, Solitons Fractals*, vol. 150, Sep. 2021, Art. no. 111170.

[40] F. Wang, Z. Zheng, and Y. Yang, "Quasi-synchronization of heterogenous fractional-order dynamical networks with time-varying delay via distributed impulsive control," *Chaos, Solitons Fractals*, vol. 142, Jan. 2021, Art. no. 110465.

[41] R. M. D. Loembe-Souamy, G.-P. Jiang, C.-X. Fan, and X.-W. Wang, "Chaos synchronization of two chaotic nonlinear gyros using backstepping design," *Math. Problems Eng.*, vol. 2015, no. 1, pp. 1–6, 2015.

[42] A. A. Kuz'menko, "Forced sliding mode control for chaotic systems synchronization," *Nonlinear Dyn.*, vol. 109, no. 3, pp. 1763–1775, Aug. 2022.

[43] F. Wang, B. Chen, X. Liu, and C. Lin, "Finite-time adaptive fuzzy tracking control design for nonlinear systems," *IEEE Trans. Fuzzy Syst.*, vol. 26, no. 3, pp. 1207–1216, Jun. 2018.

[44] H. Wang, B. Chen, C. Lin, Y. Sun, and F. Wang, "Adaptive finite-time control for a class of uncertain high-order non-linear systems based on fuzzy approximation," *IET Control Theory Appl.*, vol. 11, no. 5, pp. 677–684, Mar. 2017.

[45] H. Su, R. Luo, J. Fu, and M. Huang, "Fixed time stability of a class of chaotic systems with disturbances by using sliding mode control," *ISA Trans.*, vol. 118, pp. 75–82, Dec. 2021.

[46] G. Hardy, J. Littlewood, and G. Polya, *Inequalities*. Cambridge, U.K.: Cambridge Univ. Press, 1952.

[47] S. Vaidyanathan, A. Sambas, and S. Zhang, "A new 4-D dynamical system exhibiting chaos with a line of rest points, its synchronizationand circuit model," *Arch. Control Sci.*, vol. 29, no. 3, pp. 485–506, 2019.

[48] B. Deng, K. Shao, and H. Zhao, "Adaptive second order recursive terminal sliding mode control for a four-wheel independent Steer-by-Wire system," *IEEE Access*, vol. 8, pp. 75936–75945, 2020.

[49] Z. Xu, W. Huang, Z. Li, L. Hu, and P. Lu, "Nonlinear nonsingular fast terminal sliding mode control using deep deterministic policy gradient," *Appl. Sci.*, vol. 11, no. 10, p. 4685, May 2021.

[50] N. Wongvanich, N. Roongmuanpha, and W. Tangsrirat, "Extended exploration grey wolf optimization, CFOA-based circuit implementation of the sigr function and its applications in finite-time terminal sliding mode control," *IEEE Access*, vol. 11, pp. 88388–88402, 2023.

[51] W. Long, J. Jiao, X. Liang, and M. Tang, "An exploration-enhanced grey wolf optimizer to solve high-dimensional numerical optimization," *Eng. Appl. Artif. Intell.*, vol. 68, pp. 63–80, Feb. 2018.

[52] S. Vaidyanathan, "Analysis, adaptive control and synchronization of a novel 4-D hyperchaotic hyperjerk system via backstepping control method," *Arch. Control Sci.*, vol. 26, no. 3, pp. 311–338, Sep. 2016.

[53] S. Franco, *Design With Operational Amplifiers and Analog Integrated Circuits*. New York, NY, USA: McGraw-Hill, 2015.

[54] *JFET Input Operational Amplifiers, LF357 Datasheet*, Nat. Semiconductor, Santa Clara, CA, USA, 2001.

[55] *Low Cost Analog Multiplier, AD633 Datasheet*, Analog Devices, Wilmington, MA, USA, 1999.

NAPASOOL WONGVANICH (Member, IEEE) received the B.E. (Hons.) and Ph.D. degrees in electrical and electronics engineering from the University of Canterbury, Christchurch, New Zealand, in 2008 and 2016, respectively.

He has been with the Department of Instrumentation and Control Engineering, King Mongkut's Institute of Technology Ladkrabang, since 2016, where he is currently an Assistant Professor. His current research interests include modeling and system identification, optimal and nonlinear control for industrial electronics, robotics, and biomedical applications.

Dr. Wongvanich served as the Treasurer for the IEEE Control Systems Society Thailand, since 2022.

PITCHAYANIN MOONMUANG received the B.Eng. degree (Hons.) in electronics engineering, the M.Eng. degree in control engineering, and the D.Eng. degree in electrical engineering from the School of Engineering, King Mongkut's Institute of Technology Ladkrabang (KMITL), Bangkok, Thailand, in 2016, 2019, and 2023, respectively. Since 2023, she has been a Lecturer with the School of International and Interdisciplinary Engineering (SIIE). Her current research interests include immittance function simulators and active analog filter design, and analog signal processing circuits and applications.

NATCHANAI ROONGMUANPHA received the B.Eng. degree in electronics engineering, the M.Eng. degree in control engineering, and the D.Eng. degree in electrical engineering from the School of Engineering, King Mongkut's Institute of Technology Ladkrabang (KMITL), Bangkok, Thailand, in 2016, 2019, and 2023, respectively. He is currently a Lecturer with the Department of Computer Engineering. His main research interests include immittance function simulators, active analog filters, oscillator design, and chaotic circuit realizations.

WORAPONG TANGSRIRAT received the B.Ind.Tech. degree (Hons.) in electronics engineering and the M.Eng. and D.Eng. degrees in electrical engineering from the Faculty of Engineering, King Mongkut's Institute of Technology Ladkrabang (KMITL), Bangkok, Thailand, in 1991, 1997, and 2003, respectively.

Since 1995, he has been a Faculty Member with KMITL, where he is currently a Full Professor of electrical engineering with the Department of Instrumentation and Control Engineering. He has edited or written 15 books and has published more than 140 research articles in many peer-reviewed international journals. His primary research interests include analog signal processing and integrated circuits, current-mode circuits, active filter and oscillator design, electronic instrumentation and control systems, and chaotic synchronization and control.

Prof. Tangsrirat has accomplished a noteworthy milestone by being consistently ranked in the ''Top 2% List of the World's Scientists'' both in terms of research impact for the career-long achievement and the most recent single year, in 2023.

∙ ∙ ∙